Available online at www.sciencedirect.com

ScienceDirect

Energy Procedia 114 (2017) 5430 – 5437

Energy Procedia

13th International Conference on Greenhouse Gas Control Technologies, GHGT-13, 14-18 November 2016, Lausanne, Switzerland

Study on dissolution process of liquid CO_2 into water under high pressure condition for CCS

Xiao Ma[a,*], Yutaka Abe[a], Akiko Kaneko[a], Shuhei Fujimoto[b], Chikahisa Murakami[b]

[a]*University of Tsukuba, 1-1-1 Tennnoudai, Tsukuba, Ibaraki 305-8573, Japan*
[b]*National Maritime Research Institute, 6-38-1 Shinkawa, Mitaka, Tokyo 181-0004, Japan*

Abstract

The objective of the present study is set as to clarify the dissolution phenomena of liquid CO_2 in the high pressure corresponding to deep-ocean, and CO_2 concentration profile near the water-liquid CO_2 interface when CO_2 hydrate formation. First of all, visualization unit is constructed which can be observed from all angles. Second, mass transfer coefficient and the solubility of CO_2 with time were calculated via volume change of gas CO_2, liquid CO_2 and dissolution water by using image processing. As a result, CO_2 mass transfer coefficient decreased with time, and solubility of CO_2 increased with time. Finally, CO_2 solubility calculated by the present study was compared to a previous study, and its indicated good agreement with the previous value of hydrate formation condition which the temperature under 10 °C.

Peer-review under responsibility of the organizing committee of GHGT-13.

Keywords: Dissolution; Vizualization observation; Mass transfer; Ocean storage

1. Introduction

Carbon dioxide capture and storage technologies were now considered one of the powerful tool to mitigate the global warming program. Especially, it is considered that ocean storage technology has 10,000 times ability than the technology to store the CO_2 underground [1]. When CO_2 is stored under the deep ocean, e.g. on the deep sea floor or under the sea bed, it can be thought that CO_2 clathrate hydrate will be formed. It is because deep-ocean satisfy the

* Corresponding author. Tel.: +81-29-853-5268; fax: +81-29-853-5487.
E-mail address: s1530208@u.tsukuba.ac.jp

Peer-review under responsibility of the organizing committee of GHGT-13.
doi:10.1016/j.egypro.2017.03.1687

formation condition for CO_2 hydrate at low temperature and high pressure [2]. Brewer et al. [3] did field study to visualize the formation of CO_2 hydrate at actual sea condition at Monterey Bay. As the result, CO_2 hydrate was actually observed at the beaker over the liquid CO_2 and pH change by CO_2 hydrate was measured. On the other hand, several experimental studies at lab scale was done and reviewed by Mori [4]. However, some model exists with an assumption which have not been evaluated its validity yet. One of the important property for developing the formation and growth of CO_2 hydrate, the solubility of CO_2 has been measured at previous study [5-8]. Ma et al. [9] observed the formation of CO_2 hydrate at the interface of liquid CO_2 and water, and the velocity of area explanation of CO_2 hydrate was calculated. Moreover, the prediction model to calculate the initial film thickness of CO_2 hydrate immediately following covering the interface was developed using results of above previous studies and a boundary layer thickness of CO_2 concentration. Although the time change of boundary layer thickness at formation of CO_2 hydrate did not measured, and the relation between boundary layer and CO_2 hydrate at hydrate formation process at unsteady condition is now unknown.

In this study, in order to clarify the formation mechanism, visualization apparatus was set up and the dissolution process of CO_2 was first measured at high pressure condition which over 45 bar. Continuously, some physical quantity were measured by image processing.

2. Experiment

2.1. Experimental apparatus

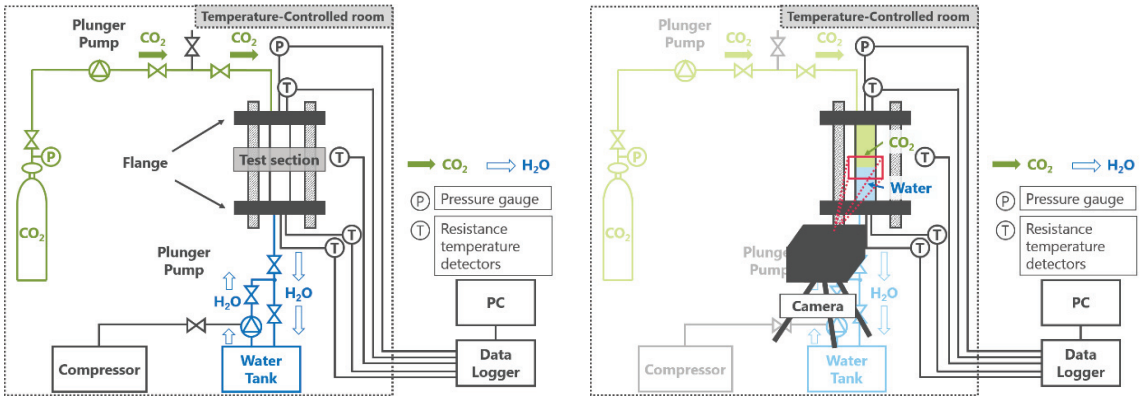

(a) schematic of the experimental apparatus (b) camera position

Fig. 1. Shematic of the experimental apparatus

Figure 1 shows a schematic image of an experimental apparatus. Figure 1(a) is a diagram of plumbing at the present study. The unit is composed by plunger pumps, resistance temperature detectors, a CO_2 cylinder, a pressure gage, a water tank, valves, flanges and a test section. In the present study, a test section is made of acrylic and it can be observed from all angles. The acrylic block is secured via flanges set at the top and bottom of the block. The test section is formed by block with circular cylinder at the center, and the inner diameter is 40 mm, height of the block is 150 mm. Resistance temperature detectors measured three points that are room temperature near the test section, a temperature of liquid CO_2 which installed top of the flange, and water temperature installed bottom of the flange. In order to keep and regulate temperature condition, all components were put in a temperature-controlled room. The video camera was also set into the temperature-controlled room and positioned a bit in front of the test section to record a dissolution phenomenon of CO_2 at high pressure condition as Fig. 1(b).

PC which placed outside of the temperature-controlled room record the digital data transfer from pressure gauge and resistance temperature detectors inside the room during the experiment.

2.2. Experimental procedure and experimental condition

First, the water was filled into the acrylic block until about the middle. Then, water had been colored by pH indicator (phenol red or methyl red). Second, gas CO_2 filled the test section and pipeline from a CO_2 cylinder. At this time, dissolution phenomena of CO_2 into the water via color change of pH indicator were observed.

After confirming that color of dissolution water with pH detector did not change, pressure at test section was pressurized by plunger pump and liquidized gas CO_2 till specific volume. Then, experimental condition was set 2 patterns. First, the condition was kept vapor-liquid coexistence that gas CO_2 and liquid CO_2 existed over distilled water. In this condition, the pressure at the test section indicate the same value during the experiment. The other condition, experimental pressure has exceeded the coexistence pressure and liquid CO_2 was filled in the test section. In this section, the pressure reached perfect liquid CO_2 phase and placed over a distilled water. After that, valves around test section was closed and position changes with time at each interface was photographed by a video camera. At the only liquid CO_2 condition, liquid CO_2 was pressed into the test section till the pressure reached to the initial pressure condition when pressure drop by CO_2 dissolution in water occurred. The experimental temperature condition was set 2.5, 4.5, 13.2, 17.1 °C, pressure condition was set 4, 6, 7 MPa. In the present condition, water density is still larger than CO_2 density. Each temperature and pressure data were recorded at every 5 seconds. The experiment finished within 18 hours at longest.

3. Result and discussion

3.1. Visualization result

Figure 2 shows the experimental result of dissolution phenomena of the gas CO_2 with time at 6 °C, 4 MPa and pH detector was used Methyl red. Figure 2(a) is the initial condition of distilled water with dissolved pH detector was set in the acrylic test section with air. At (b), CO_2 gas filled the test section and then a color at the interface of gas CO_2 – distilled water was changed and indicated pH beginning to decrease. At (c) to (f), it can be observed that the red area which indicated low pH region was expanded with time. At the same time, liquefied CO_2 was observed at the interface between gas CO_2 and distilled water. It is because the condition in CO_2 cylinder is in a vapor-liquid coexistence of CO_2 and a pressure in the test section reached the coexistence condition similar CO_2 cylinder. After (f), it was observed that the color change rate was decreased at (g) and the color change did not observe at (h). Reaction ranges of pH of Methyl red is 4.4 – 6.5 and it can be thought pH in dissolution water exceed the value 4.4 within 10 seconds at longest.

Figure 3 shows the picture shoot at 160 minutes from Fig. 2 at 6 °C and 4 MPa condition. As the result, area of gas CO_2 and dissolution water was increasing with time. On the other hand, it was observed region of liquid CO_2 was decreasing with time. The dissolution rate of each phase was calculated quantitatively at the next section.

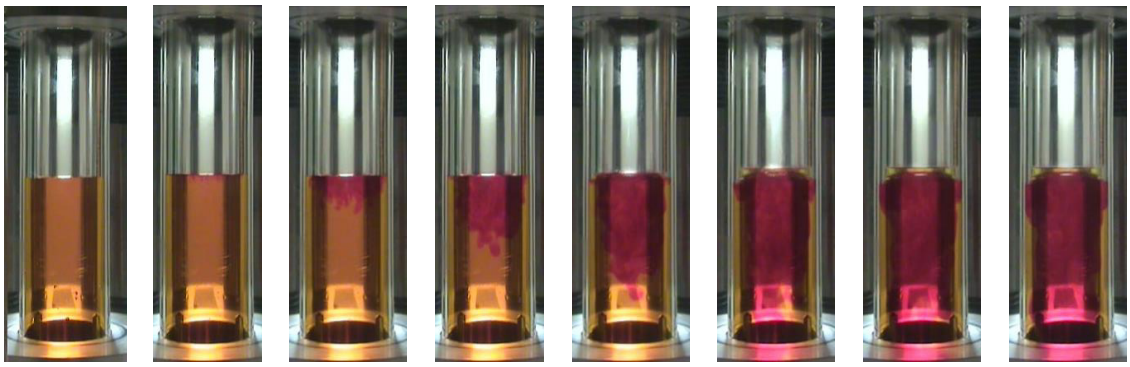

(a) t = 0 s (b) t = 5 s (c) t = 6 s (d) t = 7 s (e) t = 8 s (f) t = 9 s (g) t = 10 s (h) t = 11 s

Fig. 2. Visualization of dissolution of gas CO_2 into distilled water at 6 °C, 4 MPa

Fig. 3. Visualizaiton result of the test section

3.2. Image processing

In order to evaluate dissolution phenomena quantitatively, a time-space diagram was created. At Fig. 4(a), one pixel at the center of test section as Fig. 3 at t=0 was extracted and lined up the pixel along the time change for right. As the result, created time-space diagram was shown in Fig. 4(a). From the top, the diagram shows the time change of volume of gas CO_2, position of gas CO_2 and liquid interface, volume of liquid CO_2, position of liquid CO_2 and water interface, water volume. Then to tracing each interface, digital image was converted BMP file format into an HSV file format and using Hue image. In consequence, the interfaces were traced perfectly as shown in Fig. 4(b). From the top, each line traced the interface between gas and liquid CO_2, between liquid CO_2 and water at center of the test section, between the interface of liquid CO_2 and water on the inside wall of the section.

Subsequently, volume of liquid CO_2, dissolution water, gas CO_2 at each time was calculated from above obtained position using time-space diagram. Then, because of different interfacial tension between liquid CO_2 and water, water volume seems convex upward. Therefore, water volume was calculated using follow Eq. (1):

$$V_{\mathrm{water}}(t) = \frac{1}{2}\frac{4}{3}\pi\left(\frac{D}{2}\right)^2 L + \pi\left(\frac{D}{2}\right)^2 (H - L) \quad . \tag{1}$$

Where, D is a diameter of the inter cylinder of acrylic block (= 40 mm), L is a height of interface of liquid CO_2 and dissolution water from the bottom of the acrylic at inside wall, H is same height of the above interface from bottom at the center which top of convex upward. Volume of liquid CO_2 was calculated as follows. Eq. (2-1) is used when the experimental condition without gas CO_2 which include only liquid CO_2 and water, and Eq.(2-2) is used with gas CO_2 condition.

$$V_{\mathrm{CO_2}}(t) = V_{\mathrm{test}} - V_{\mathrm{water}}(t) \qquad (\text{without gas } \mathrm{CO_2} \text{ region}) \tag{2-1}$$

$$V_{\mathrm{CO_2}}(t) = \pi\left(\frac{D}{2}\right)^2 \big(h(t) - H(t)\big) - V_{\mathrm{water}}(t) \quad (\text{with gas } \mathrm{CO_2} \text{ region}) \tag{2-2}$$

Where, V_{test} is the volume of test section that circular cylinder inside an acrylic block (= about 188,496 mm^3), h is the height of the interface between liquid CO_2 and gas CO_2 from the bottom. Next, a time change of mass and volume were calculated. Each value of dissolution water and liquid CO_2 was calculated using follow equations Eq. (3) and (4). Mass of dissolution water was calculated as the summation of initial distilled water filled in the test section and dissolved liquid CO_2 at each time. On the other hand, mass of liquid CO_2 at a time t is calculated as a difference between initial mass and dissolved mass as above.

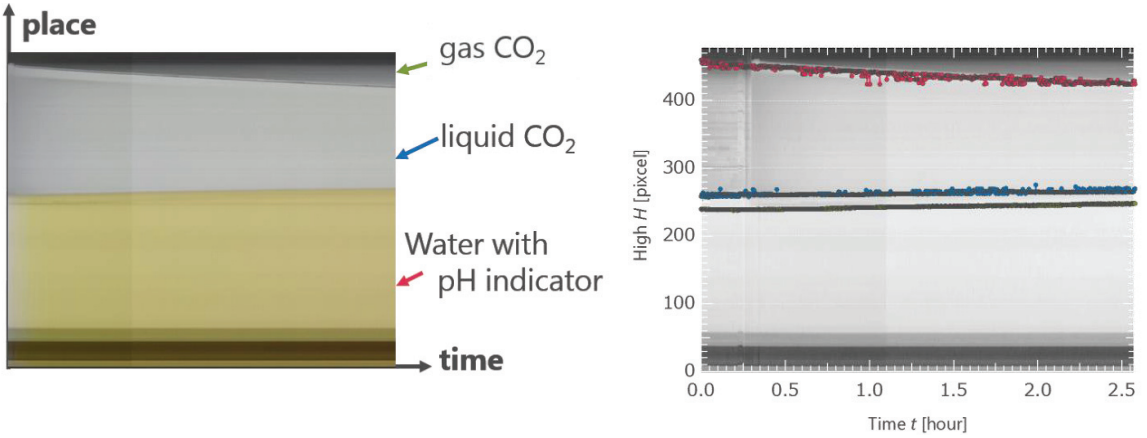

(a) time-space diagram (b) HSV converged picture and result of interface tracking

Fig. 4. Time-space diagram and the tracing result of each interface

$$M_{\text{water}}(t) = M_{\text{water}}^{\text{initial}} + \rho_{CO_2} \cdot \Delta V_{CO_2}(t) \tag{3}$$

$$M_{CO_2}(t) = M_{CO_2}^{\text{initial}} - \rho_{CO_2} \cdot \Delta V_{CO_2}(t) \tag{4}$$

Where, V_{CO2} is dissolved volume of liquid CO_2 from an initial time using time-space diagram, ρ_{CO2} is a density of liquid CO_2 at an experimental condition. Obtained each time change of volume and mass is shown in Fig. 5. The vertical axis of left is volume of dissolution water and liquid CO_2, and the right axis is the dissolution rate of liquid CO_2. The time change of mass of both dissolution water and CO2 was corresponding to the volume change at each time. Then, the concentration of CO_2 in bulk water was calculated with dissolved CO_2 mass divided by volume of dissolution water at each time using Eq. (5). Continuously, dissolution rate of liquid CO_2 was calculated by Eq. (6).

$$C_{CO_2}^{\text{bulk}} = \frac{\Delta M_{CO_2}(t)}{V_{\text{water}}(t)} \tag{5}$$

$$v_{CO_2} = \frac{dM_{CO_2}}{dt} \tag{6}$$

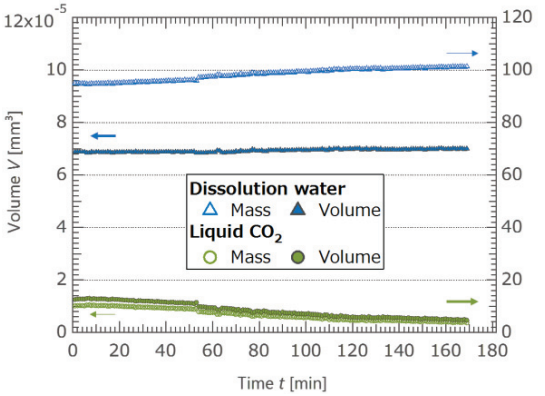

Fig. 5. Mass change of the liquid CO_2 and the dissolution water

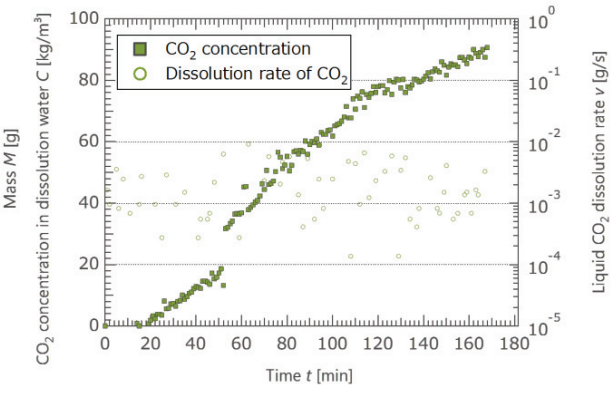

Fig. 6. CO_2 concentration change and dissolution rate of CO_2

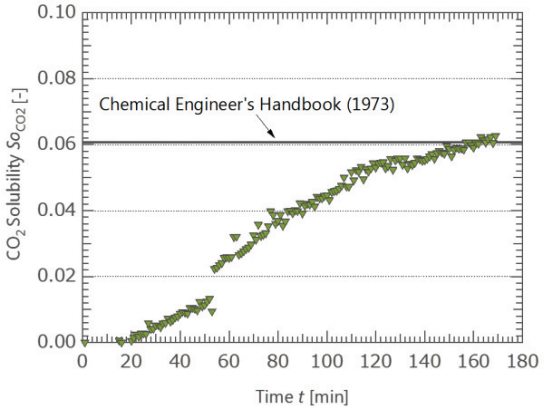

Fig. 7. CO_2 solubility change

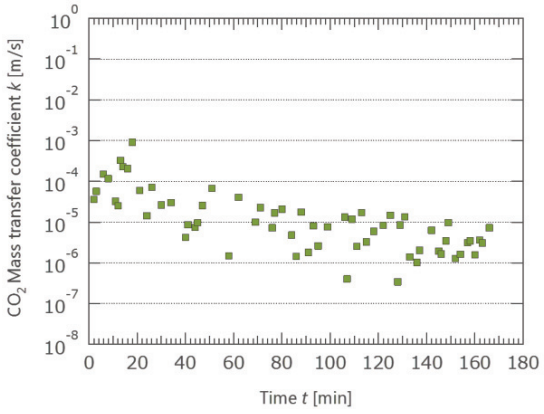

Fig. 8. CO_2 Mass transfer coefficient

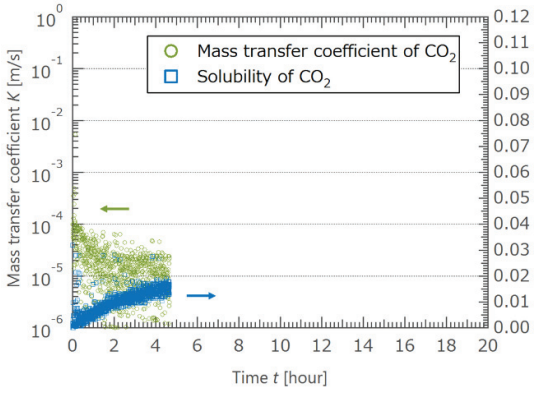

(a) 13.2 °C, 6 MPa, without CO_2 gas

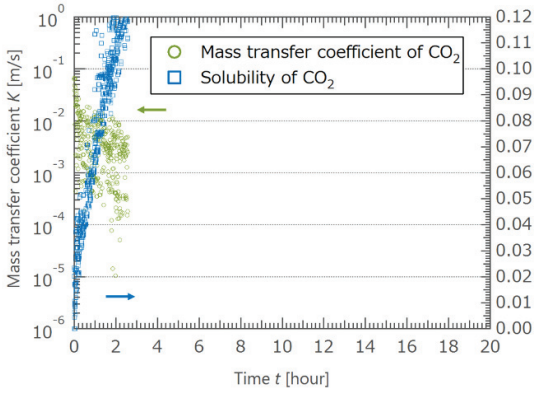

(b) 13.2 °C, 4 MPa, with CO_2 gas

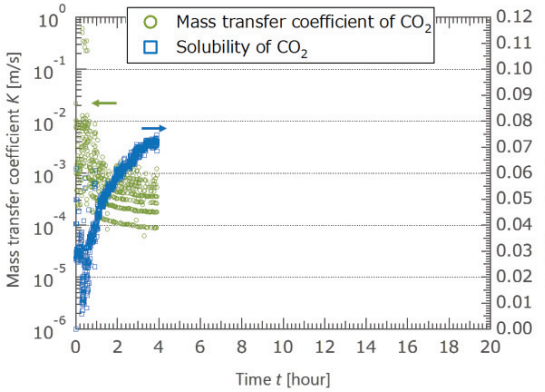

(c) 4.5 °C, 6 MPa, with CO_2 gas

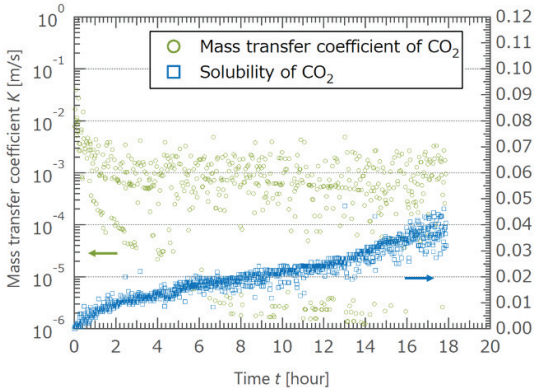

(d) 2.5 °C, 7 MPa, without CO_2 gas, with Hydrate

Fig. 9. Mass transfer coefficient and solubility of CO_2 in water with time at each experimental condition

These values with time was shown in Fig. 6. The vertical axis of left is CO_2 concentration, and the axis of right is dissolution rate of liquid CO_2. As the result, it can be confirmed that the concentration increased with time and reached to the saturated condition. On the other hand, the dissolution rate of CO_2 approximately kept the order between 10^{-4} to 10^{-2} g/s from the initial condition of 6 °C and 4 MPa.

Using calculated above some physical values, CO_2 solubility in water and CO_2 mass transfer coefficient at liquid CO_2 and water interface is now calculated. Each equation was described as follows Eq. (7), (8).

$$So_{CO_2} = \frac{\Delta M_{CO_2}}{M_{water}} \tag{7}$$

$$k_{CO_2} = \frac{1}{A}\frac{dM_{CO_2}}{dt}\frac{1}{\rho_{CO_2} \cdot So_{CO_2}(t) - C_{CO_2}^{bulk}} \tag{8}$$

Where, A is an area of the test section (= about 1257 mm^2). Figure 7 and 8 shows above time change of CO_2 solubility and mass transfer coefficient. As a result of calculation a solubility and mass transfer coefficient of CO_2, solubility increased with time and mass transfer coefficient decreased with time. It can be thought that CO_2 dissolved well into a water at the initial condition because there are no CO_2 in water. After the interface of liquid CO_2 and water was created, mass transfer coefficient decreased with CO_2 concentration increased. Calculated solubility of CO_2 was increased and reached the value similar to the value of Chemical Engineer's Handbook at same condition. Therefore, it was confirmed that the experimental result indicated the validity of the present experimental system and experimental result.

As is the case with above Eq. (1) to (8), solubility and mass transfer coefficient of CO_2 with time was calculated at some experimental conditions. These value changes with time was described in Fig.9 then the vertical axis of all figure is set the solubility of CO_2, and the right axis of all figure is set mass transfer coefficient of CO_2. At Fig. 9(a) and (d), the experimental condition did not include gas CO_2 and CO_2 hydrate film was confirmed at condition of Fig. 9(d). On the other hand, Fig. 9(b) and (c) included gas CO_2 in addition to liquid CO_2 and water. As the result, mass transfer coefficient was obtained in the order of 10^{-4} to 10^{-6} m/s. Compared to previous study measured mass transfer coefficient of CO_2 by Aya et al. [8], calculated value of the present study is 10 or 10^2 times larger than their value. On the other hand, calculated solubility at the experiment finished was plotted with previous study in Fig. 10. As a result, values at Fig. 7 agreed with previous study at no-hydrate existence temperature (over 10 °C) condition. Similarly, Fig. 9(c) and 9(d) agreed with previous study at hydration temperature (under 10 ˚C) with the observation of CO_2 hydrate film. At Fig. 9(a) and (b), CO_2 solubility of the present study is different from measured value at previous studies [5-8]. At these conditions, hydrate will not be formed. The value of Fig. 9(a) is much smaller than numerical dashed line. It can be thought the experiment needed more experimental time on the condition and dissolution water has not been reached the saturation condition.

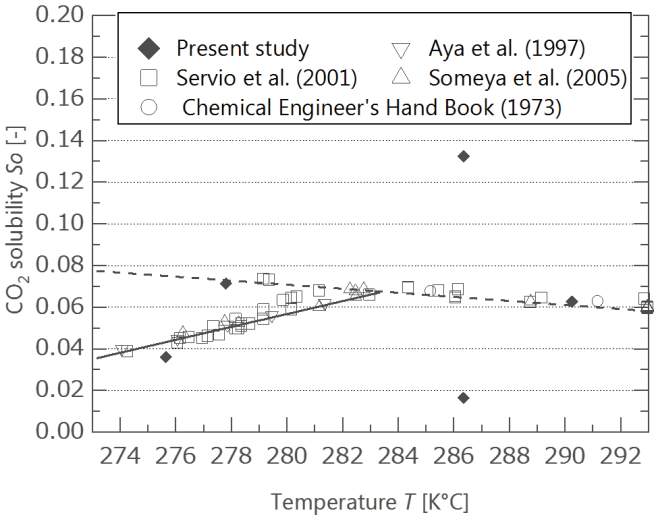

Fig. 10. Calculated saturated concentration of CO_2 in water. The dash line means the solubility at without CO_2 hydrate condition, and the solid line means the solubility with CO_2 hydrate condition by least square approximation.

4. Conclusions

1. Visualization unit for high pressure was produced and dissolution phenomena of CO_2 were observed at two phase condition (liquid CO_2 and water) and three phase condition (gas CO_2, liquid CO2 and water). When gas CO_2 filled in the test section, water with pH detector changed immediately within at longest 10 seconds.

2. After the concentration of CO_2 in water exceeded the reaction range of pH detector, pressure was increased and CO_2 was liquidized at the test section. In both conditions of with gas CO_2 and without gas CO_2, water region increased with time. At with gas CO_2 condition, volume change of liquid CO_2 was observed and it decreased with time.

3. By image processing for photographing pictures, the interface of liquid CO_2 and gas CO_2, the interface of liquid CO_2 and dissolution water was traced perfectly. Using the position of interfaces, each physical quantity change with time, e.g. the volume of each phase, mass of liquid CO_2, CO_2 concentration in the water, dissolution rate, solubility of CO_2, and mass transfer coefficient, was calculated.

4. Compared to previous studies, final CO_2 solubility when the experiment has finished was calculated from the present study. These values agreed with the value of the previous experimental study especially at hydration temperature condition. In addition, mass transfer coefficient indicates the order between $10^{-6} \sim 10^{-4}$ m^2/s.

References

[1] Bergman PE, Piemer PE, Wokaun A. Geological sequestration of CO_2. Astatus report. Greenhouse Gas Control Technologies 2000;p.167-173.
[2] Sloan ED, Koh CA. Clathrate Hydrates of Natural Gases. 3rd ed. Boca Raton: CRC Press, 2007.
[3] Brewer PG, Edward TP, Gernot F, Aya I, Yamane K. Experiments on the ocean sequestration of fossil fuel CO_2: pH measurements and hydrate formation. Marine Chemistry 2000;72.p.52-93.
[4] Mori YH. Clathrate hydrate formation at the interface between liquid CO_2 and water phases – A review of rival models characterizing “Hydrate films”. Energy Convers. Mgmt 1998;39: 15.p.1537-1557.
[5] Perry RH, Chilton CH. Chemical engineer’s Handbook, New York: McGraw-Hill Book Company, 1973.
[6] Servio P, Englezos P. Effect of temperature and pressure on the solubility of carbon dioxide in water in the presence of gas hydrate. Fluid Phase Equilibria 2001;190.p.127-134.
[7] Someya S, Bando S, Chen B, Song Y, Nishio M. Measurement of CO_2 solubility in pure water and the pressure effect on it in the presence of clathrate hydrate, International Journal of Heat and Mass Transfer 2005;48.p.2503-2507.
[8] Aya I, Yamane K, Nariai H, Solubility of CO_2 and Density of CO_2 Hydrate at 30MPa. Energy 1997;22:2/3.p.263-271.
[9] Ma X, Abe Y, Kaneko A, Yamane K. Mass Transport Properties on Time Series Variation of CO_2 Hydrate Film. Energy Procedia 2014;63.p.5925-5932.